Proceedings of the ASME 2010 3rd Joint US-European Fluids Engineering Summer Meeting and 8th International Conference on Nanochannels, Microchannels, and Minichannels
FEDSM-ICNMM2010
August 1-5, 2010, Montreal, Canada

FEDSM-ICNMM2010-31071

INVESTIGATION OF POD BASES FOR FLOW CONTROL ON DISK WAKES

Zachary Berger
L.C. Smith College of Engineering
and Computer Science
Department of Mechanical and Aerospace Engineering
Syracuse University, Syracuse, NY 13210

Rory Bigger, Makan Fardad
Hiroshi Higuch, Mark N. Glauser, Aaron J. Orbaker
L.C. Smith College of Engineering
and Computer Science
Department of Mechanical and Aerospace Engineering
Syracuse University, Syracuse, NY 13210

ABSTRACT

This work investigates the effects of flow control on the near wake region of a disk in a water flow, utilizing the POD reconstructed time dependent velocity fields. Velocity measurements were collected using time resolved particle image velocimetry (TRPIV) at a Reynolds number of 20,000 based on the disk diameter, both with and without control. An open-loop control was applied via periodic synthetic jet excitation from the disk edge. With the advantage of a time resolved velocity database, we have the ability to reconstruct the time dependent velocity field in the wake of the disk. This reconstruction is done for the baseline and controlled cases using various POD truncations to observe velocity reconstructions, based on the overall energy of the system. In doing so, we will consider the convergence rate of the spatial eigenvalues when conducting our POD reconstruction of the fluctuating velocity field, for both the baseline and controlled cases.

Since a complex flow exists in the wake of the disk, the goal will be to form a state space representation of the flow in the form of a linear time invariant (LTI) system. This model is simply a linearization of the flow around the baseline. Furthermore, our knowledge of the input control signal will allow us to predict the flow at a later instant in time. We would like to extract the most energetic modes of the system and thereby form our observer-based controller to close the loop. In order to accomplish this, and with a rich open-loop dataset at our disposal, we will first form the POD reconstruction of the baseline. We then form a new basis, obtained by taking the actuated (controlled) data and subtracting from it the components of the flow that fall in the subspace spanned by the baseline flow. This will characterize the flow field by capturing the effect of the control input (actuation), from which the parameters of the LTI system can be identified. Preliminary POD reconstruction shows that 60% of the energy is recovered from 20 POD modes of the total 511 modes for the baseline case; similarly 60% of the energy is also recovered from 100 POD modes of the total 1,024 modes for the actuated case.

INTRODUCTION

The goal of this work is to control the wake behind a three dimensional bluff body, which in this particular case is a disk. We will investigate the behavior of the flow around a disk in a water channel, while implementing time resolved PIV to acquire velocity measurements. In addition, we implement a piston and cylinder configuration external to the flow for flow control. The current test bed data set provides us with a rich, open loop, time-resolved PIV database of the flow in the near wake region of the disk. The data was acquired by Bigger et al [1] and involves a 0.120 m diameter disk, at a Reynolds number (Re) = 20,000, tested in a wind tunnel and water channel with actuation input at the disk's edge. We refer to the data collected in the water channel where time-resolved PIV was implemented to capture the velocity field in the wake of the disk. We have been exploring various methodologies that incorporate reduced order mod-

eling techniques, i.e. Proper Orthogonal Decomposition (POD), so that we may ultimately establish closed loop control.

Motivation

When examining bluff body flow separation, whether it is incipient or massive separation, studies have been performed which validate that flow control has the potential to be a key solution to these types of problems. Previous work by Bigger et al [1] has shown that the wake behind an axisymmetric bluff body can be altered using open-loop active flow control. Here it is discussed that in order to control the flow over a sphere, open loop control will cause a delay in flow separation, a smaller wake region and reduce the drag. In addition, a study conducted by Naim et al [2] regarding active flow control of a circular cylinder, assures that open loop control has a pronounced effect on boundary-layer transition and separation.

In the field of flow control, we see increasing evidence that there are advantages to closed loop flow control methods for certain applications. Cattafesta et al [3] verify that closed loop control can linearly stabilize a system and reduce the amplification of external disturbances, such as boundary layer turbulence. Glauser et al [4] and Pinier et al [5] discuss the positive effects of flow control for a NACA 4412 airfoil under incipient separation conditions and touch upon the energy and efficiency benefits of closed versus open loop control. Camphouse et al [6] and Wallace et al [7] describe the benefits of feedback flow control for both static and pitching turrets, respectively, in the context of reducing the adverse aero-optics effects associated with separated turbulent flows. Therefore, the task at hand is to now create a closed-loop control technique for this disk wake problem.

In order to come up with an accurate feedback controller for this flow, we will use our knowledge of the flow field along with a proper orthogonal decomposition (POD) reconstruction of the velocity field to form an observer-based controller.

We plan to investigate the fluctuating velocity field behind the disk for the baseline case (with no actuation), as well the actuated case. The overall goal in this technique is to perform snapshot POD on each of our data sets respectively so that we may extract the most energetic modes of the system and cleverly form our observer-based controller to close the loop.

FEEDBACK CONTROLLER METHODOLOGY

Since a complex flow exists in the wake of bluff bodies such as a disk, the goal will be to form a state space representation of the flow. In other words, we would like to approximate the flow field with a linear time invariant (LTI) system. The basis of this work was first proposed by Fardad [8] and will be described below.

The LTI system dealt with in this case is of the form:

$$\frac{d}{dt}\psi(t) = A\psi(t) + Bd(t) \tag{1}$$

$$p(t) = C\psi(t) \tag{2}$$

In Eqns. 1 and 2, $\psi(t)$ describes the state of the flow at any time t; d (t) characterizes the actuation input to the flow, by means of the piston cylinder system in this case. In addition p (t) is the measurement output of the system and that leaves the matrices A, B, and C, which will be described in further detail later. This model that we have just described is simply a linearization of the flow around the baseline. Of course such a model is needed because of our complex flow field induced behind the disk.

It is now our task to find the matrices A, B and C using the information of the flow field from PIV measurements along with the POD reconstructions of such measurements.

First we will use our time resolved PIV snapshots from the uncontrolled, baseline flow to form our first POD basis, which we will denote as $\phi_i(x)$. We now take the PIV snapshots of the actuated flow, denoted by $u(t,x)$, and form a new POD basis that combines the baseline POD basis and actuated snapshots. Our new basis is represented in the following way:

$$\delta u(t) = u(t) - \sum_i < u(t), \phi_i > \phi_i \tag{3}$$

The new basis, $\delta u(t)$, is obtained by taking the actuated snapshots of the flow and subtracting the components of the flow that fall in the subspace spanned by the baseline flow [8]. This is an accurate representation of the controlled, or actuated flow field.

At this point, $\delta u(t)$ is used to form a new POD basis, which will be denoted by $\eta_i(x)$. We will then retain the most energetic modes of this basis, denoted by M. We now define the following:

$$\psi_i(t) = < \delta u(t), \eta_i > \tag{4}$$

In this case $i = 1, ..., M$, where M = most energetic elements, i.e. POD modes. Therefore we say that at any time t, $\psi(t)$ characterizes the deviation of the flow from the baseline case (i.e. the state space representation of the flow).

Since the data that has been collected is in the form of time resolved PIV, then $\delta u(t)$ and $\psi(t)$ are defined at discrete time instances. So now we can define a discrete time approximation

of our continuous LTI system that we have previously described, and it is represented in the following way:

$$\psi(t+1) = A_d\,\psi(t) + B_d d(t) \tag{5}$$

$$p(t) = C_d\,\psi(t) \tag{6}$$

Equations 5 and 6 characterize the discrete time version of our continuous LTI system. The subscript d on matrices A, B, and C imply discrete time. In addition A, B, and C can be found from the discrete representations.

The next step is to find A_d and B_d using the above equations. We will do so by first taking the transpose of the above equation, term by term, keeping in mind that we are dealing with matrices.

$$\psi(t+1)^T = \psi(t)^T A_d^T + d(t)^T B_d^T \tag{7}$$

$$\psi(t+1)^T = [\psi(t)^T d(t)^T] \left| \begin{matrix} A_d^T \\ B_d^T \end{matrix} \right| \tag{8}$$

Since we have multiple snapshots in time, we can represent Eqns. 7 and 8 in the following way:

$$\left| \begin{matrix} \psi(1)^T \\ . \\ . \\ . \\ \psi(t+1)^T \end{matrix} \right| = \left| \begin{matrix} \psi(0)^T & d(0)^T \\ . & . \\ . & . \\ . & . \\ \psi(t)^T & d(t)^T \end{matrix} \right| \left| \begin{matrix} A_d^T \\ B_d^T \end{matrix} \right| \tag{9}$$

$$\left| \begin{matrix} \psi(1)^T \\ . \\ . \\ . \\ \psi(t+1)^T \end{matrix} \right| = \Omega \left| \begin{matrix} A_d^T \\ B_d^T \end{matrix} \right| \tag{10}$$

Now A_d and B_d can be computed by finding the pseudo-inverse of the matrix Ω. We also note that C_d can be found in the same way using Eqn. 6 that we have previously stated. Now that we know the state of the system, we can form an observer-based controller (i.e. Kalman filter). In other words, once the state is known, we can apply a feedback control signal to the system to formulate our closed loop control technique.

POD RECONSTRUCTION

In order to form the controller for this disk flow configuration, we must first obtain PIV snapshots of the flow field for the baseline (uncontrolled) and actuated (controlled) cases. With this database of information readily available from Bigger et al [1], the next task is to form our respective POD bases.

As our first step we will perform POD on the baseline data using the following basic technique. First, it is important to note that our result will include the fluctuating velocity, where the fluctuating velocity is simply defined as the instantaneous velocity minus the mean velocity. In addition, since time-resolved PIV is implemented, the velocity has a u and v component, with each velocity component being a function of x, y, and t, as follows:

Actual Fluctuating Velocity Field

$$u_{fluct}, v_{fluct}(x,y,t) \tag{11}$$

Likewise we can define our POD reconstruction in the following way:

$$u^m, v^m(x,y,t) = \sum_{k=1}^{m} a^k(t)\phi^k(x,y) \tag{12}$$

In Eqn. 12, m specifies the number of modes in the POD reconstruction. In addition "a" is the POD coefficient and ϕ is the eignefunction characterizing the baseline POD basis.

BASELINE RESULTS

For the baseline case with no actuation, we have a total of 511 snapshots which corresponds to a total of 511 POD modes for a full reconstruction of the velocity field. What we would like to do next is characterize the relationship between the number of POD modes and the energy of the system. A POD reconstruction of 511 modes will recover 100% of the total energy. In this next section we will look at the convergence rate of the spatial eigenvalues to see how effective our POD reconstruction is as it pertains to a recovery of the total energy of the system.

As can be seen in Figure 1, the convergence rate of the eigenvalues shows us that with as few as 20 POD modes of the original 511, over 60% of the total energy of the system is recovered. In addition, we note that 50 modes recovers over 75% of the energy and 250 modes recovers 93% of the total energy. This will prove to be very helpful when we create our baseline POD basis for our controller as discussed in the previous section.

Next we would like to compare a 20 mode POD reconstruction of the baseline velocity to the original fluctuating velocity field, which would correspond to a full 511 mode reconstruction. In addition since we have time resolved data, we can also take a

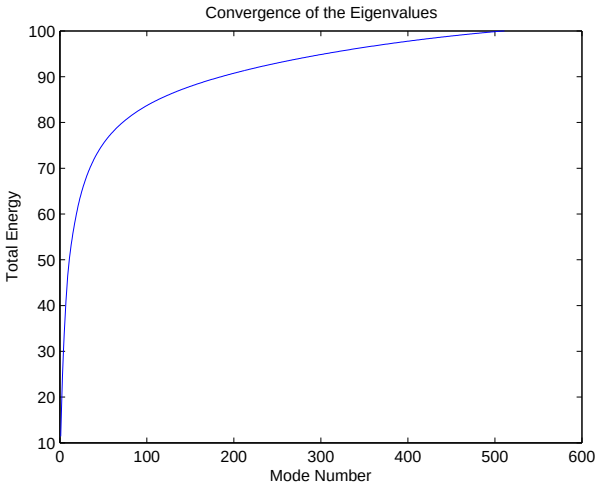

FIGURE 1. CONVERGENCE OF THE POD EIGENVALUES FOR THE BASELINE CASE

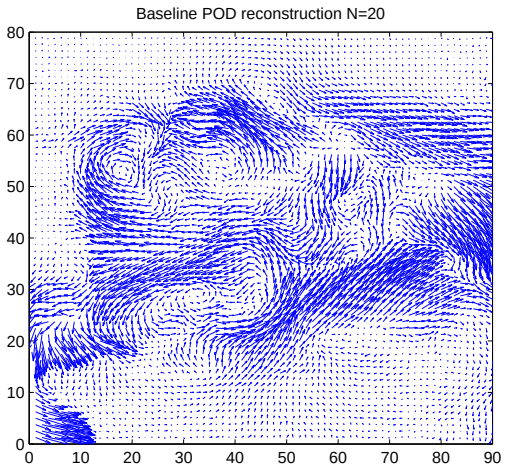

FIGURE 2. 20 MODE RECONSTRUCTION, t = 10

few snapshots throughout the experiment to see the progression of the flow through time, along with POD reconstruction.

Figures 2 through 7 characterize the baseline flow and represent the fluctuating velocity field in the wake of the disk. The disk is located in the far left-center region of the PIV window in each figure. Each pair of figures had two images, one of which is a 20 mode POD reconstruction of a particular snapshot of the experiment. The other figure in the pair is the original fluctuating velocity corresponding to the POD reconstruction in the previous figure. Figures 2 and 3 represent the 20 mode reconstruction and corresponding original fluctuating velocity field at the time

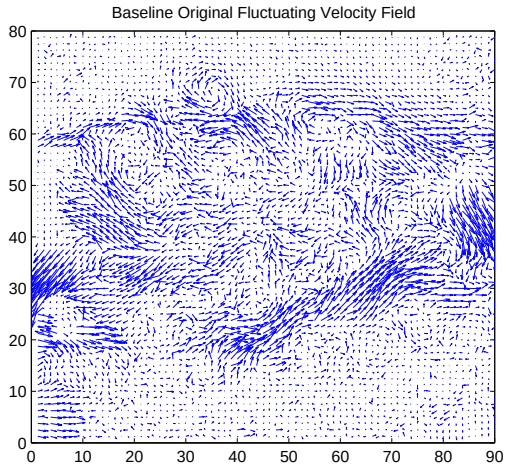

FIGURE 3. ORIGINAL FLUCTUATING VELOCITY, t = 10

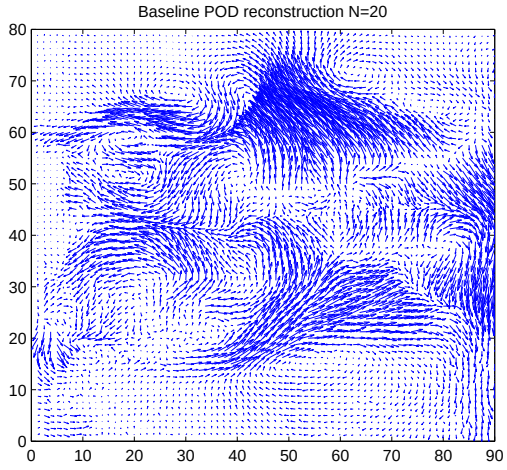

FIGURE 4. 20 MODE RECONSTRUCTION, t = 300

snapshot t = 10.

Figures 4 and 5 are similar except they correspond to the snapshot t = 300. Likewise figures 6 and 7 correspond to the snapshot t = 510. In this case, a 20 POD reconstruction of the baseline corresponds to 60% of the total energy of the flow. Therefore in each corresponding pair of images, the same vortex structures, being shed off of the disk, that appear in the original fluctuating velocity field can be seen in the 20 mode reconstruction. It is also important to note here that flow is traveling in the conventional direction, from left to right in the PIV window. Now we will take a look at the actuated (controlled) case for our data.

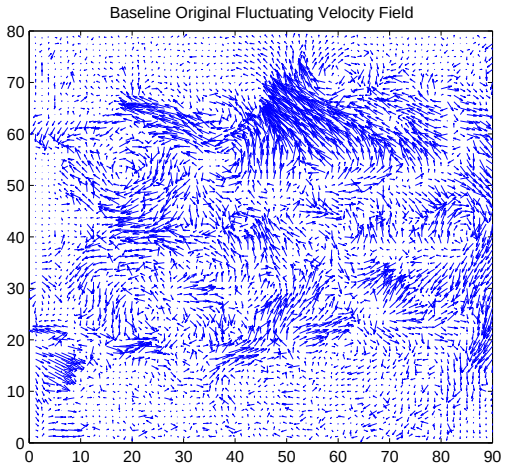

FIGURE 5. ORIGINAL FLUCTUATING VELOCITY, t = 300

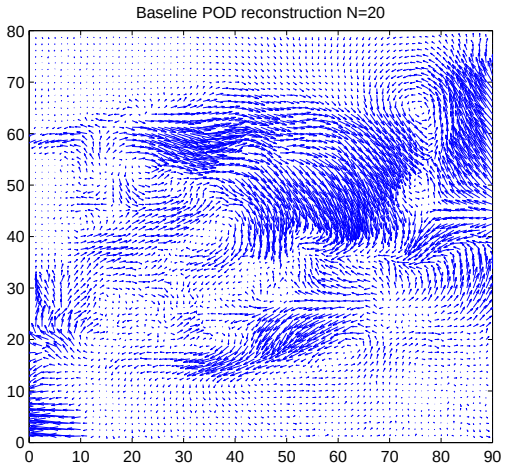

FIGURE 6. 20 MODE RECONSTRUCTION, t = 510

ACTUATED RESULTS

In Figure 8, we observe the convergence rate of the POD eigenvalues, as they relate POD modes to the total energy of the system, for the actuated case. We see here that similar to the baseline case, we have a convergence rate such that we retain 60% of the total energy with only the first 100 POD modes, out of a total of 1,024 modes. In addition, 232 modes recovers nearly 75% of the total energy and 650 modes recover about 95% of the total energy.

Similar to our representation of the baseline case, we will now show a 100 mode POD reconstruction (60% energy) and compare this with the full 1,024 mode reconstruction (original fluctuating velocity field), at 3 different snapshots (time instances) during the test.

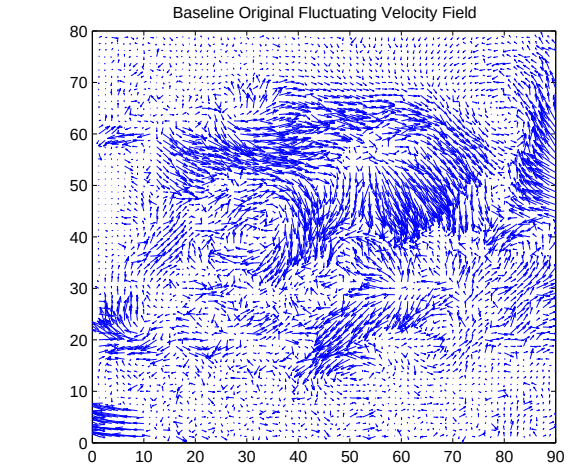

FIGURE 7. ORIGINAL FLUCTUATING VELOCITY, t = 510

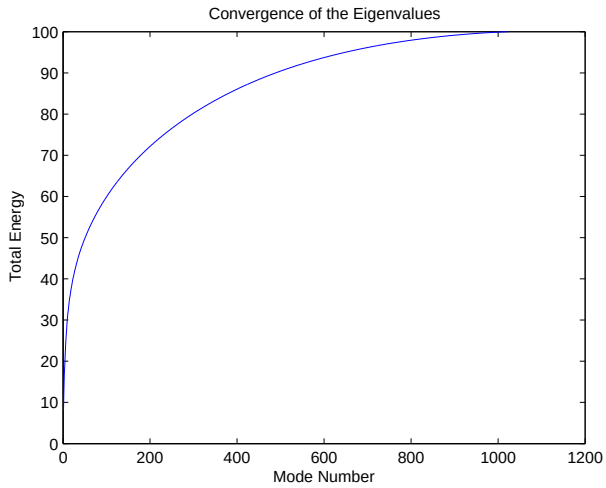

FIGURE 8. CONVERGENCE OF THE POD EIGENVALUES FOR THE ACTUATED CASE

Figures 9 through 14 show the fluctuating velocity field and the corresponding 100 mode POD reconstructions of the flow past the disk with actuation. As with the baseline case, each pair of figures characterizes the POD reconstruction and original fluctuating velocity field at different snapshot in time throughout the experiment. For each pair the first figure shows the 100 mode reconstruction and the second figure shows the full modal recon-

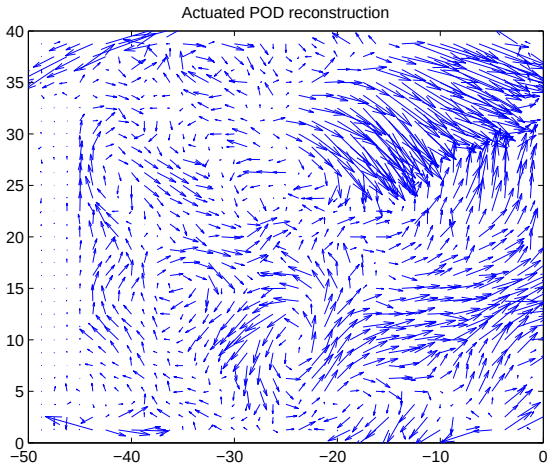

FIGURE 9. 100 MODE RECONSTRUCTION, t = 100

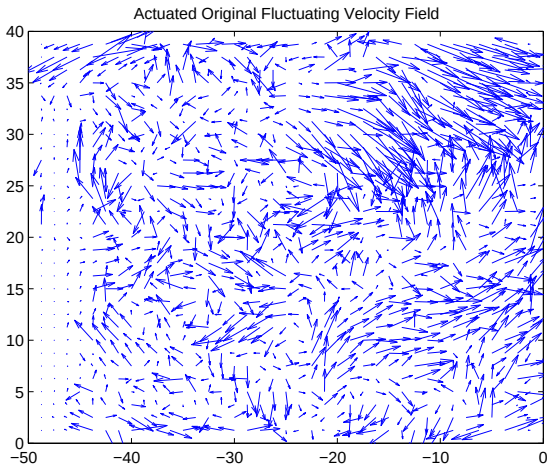

FIGURE 10. ORIGINAL FLUCTUATING VELOCITY, t = 100

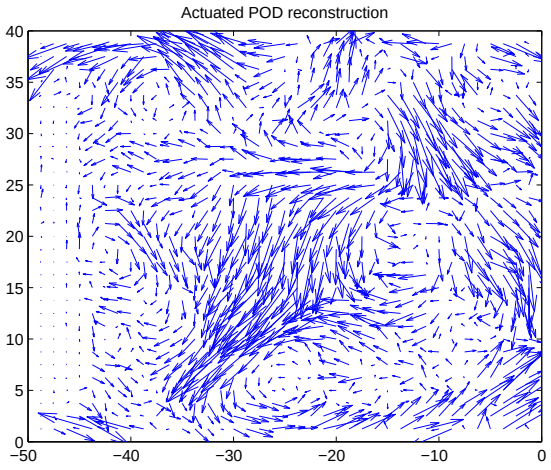

FIGURE 11. 100 MODE RECONSTRUCTION, t = 500

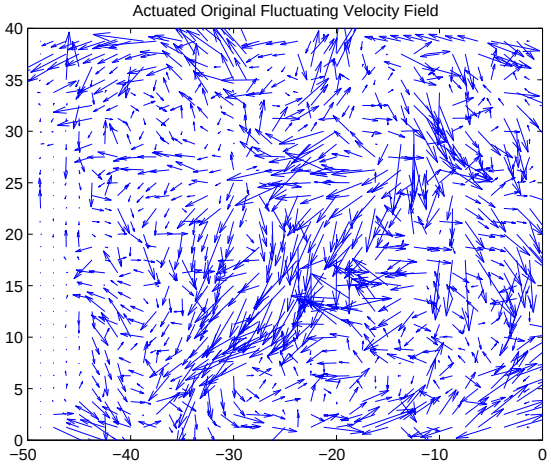

FIGURE 12. ORIGINAL FLUCTUATING VELOCITY, t = 500

struction (1,024 POD modes).

With the baseline case, 20 modes out of 511 corresponded to 60% of the total energy of the system. Likewise 100 modes out of 1,024 for the actuated case also corresponds to 60% of the total energy of the system. For the purposes of comparison, we choose the number of POD modes for both the baseline and actuated cases to reflect an energy recovery of 60%. At each snapshot (t =100, 500 and 1000), it is easy to once again observe the vortex structures in the POD reconstruction figure as they correspond to the original fluctuating velocity field. In fact, it almost becomes easier to see the vortices shedding off of the disk in the POD reconstruction images. The 100 mode reconstruction seems to ”clean up” the flow, with 60% of the total energy being recovered, in this particular case.

CONCLUSIONS

From the results shown above, it can be easily seen that there seems to be an acceptable convergence rate of the POD eigenvalues for both the baseline and actuated cases of the flow behind the disk. We have seen that for the baseline case, which consists of 511 total snapshots (POD modes), 20 POD modes recovers 60% of the total energy. In addition, for the actuated case which consists of 1,024 total snapshots (POD modes), we see that 100

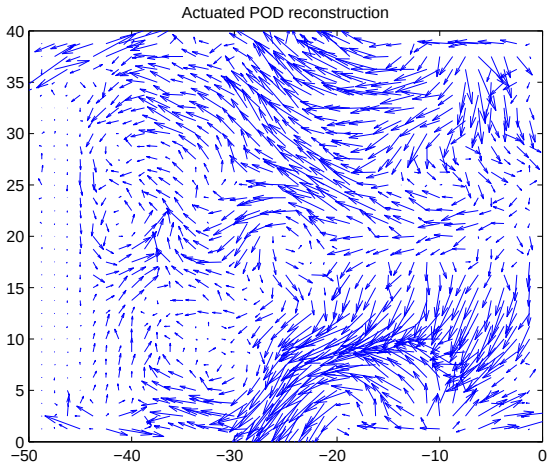

FIGURE 13. 100 MODE RECONSTRUCTION, t = 1000

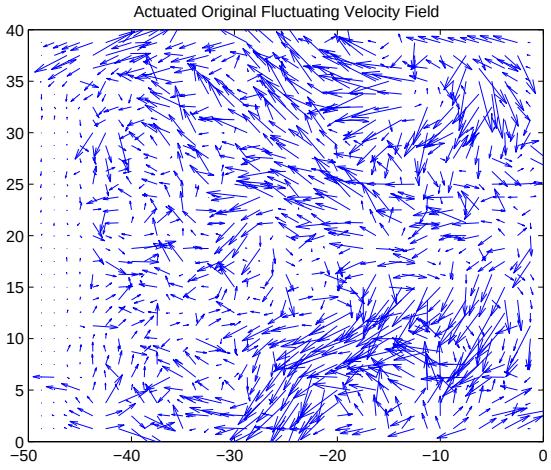

FIGURE 14. ORIGINAL FLUCTUATING VELOCITY, t = 1000

POD modes also recovers about 60% of the total energy.

From these results we are able to then represent the POD reconstructions based on the fluctuating velocity fields. We have seen that for both the baseline and actuated cases alike, we see a nice correlation in the POD reconstruction and the full modal reconstruction of the original velocity field.

With 60% of the energy recovered in our particular POD reconstruction, it is clear to see the flow physics and structures forming in the wake of the disk. In addition, we have the advantage of possessing time resolved data which allows us to see the progression of the flow through time, in both the raw data sense as well as with POD reconstructions. In time, one can even see the vortex structures behind the disk developing, which is advantageous when studying bluff body flow control as we are doing here.

When analyzing bluff body flow separation, it is important to first fully understand the flow physics associated with the problem at hand. We have taken an open loop study of the flow in the near wake region of a disk and formulated a reduced order modeling technique to establish a closed loop flow control process.

FUTURE WORK

Now that we have performed POD on our baseline data and obtained data for our actuated case, the next step is to continue with process outlined in the Feedback Controller Methodology section. We must calculate the ensemble of snapshots $\delta u(t)$, which we recall is the actuated (controlled) PIV snapshots, and subtract the POD bases from the baseline (uncontrolled) case. This will hopefully characterize the effect of the control actuation of the flow field, as we have discussed previously.

Once we have performed this task, we can then find our matrices A, B and C, in the state space equations, which will then allow us to form our controller for feedback flow control.

In addition, since this data has been previously collected, we plan on using the current test bed database simply for analysis and design of our controller. The next step is to build a new disk so that we may take new measurements and implement our closed-loop controller for further analysis. The concepts and results that we have shown and discussed in this paper are merely a stepping stone towards the overall effort in the study of closed-loop flow control for disk wakes, as well as other three dimensional bluff bodies. Our hope is that we can eventually implement our technique on other geometries that involve the application of closed loop flow control in the aerospace community and beyond.

REFERENCES

[1] Bigger, R.P., Higuchi, H., and Hall, J.W., 2009. "Open-Loop Control of Disk Wakes". *AIAA Journal*. Vol 47, No.5, May.

[2] Naim, A., Greenblatt, D., Seifert, A, and Wygnanski, I., 2007. "Active Control of a Circular Cylinder Flow at Transitional Reynolds Numbers". *Flow Turbulence Combust.*. Vol 78, p. 383-407.

[3] Cattafesta, L., Song, Q., Williams, D.R., Rowley, C.W., and Alvi, F.S.,2008. "Active Control of Flow-Induced Cavity Oscillations". *Progress in Aerospace Sciences*. Vol. 44, December, pp. 459-502.

[4] Glauser, M. N., Higuchi, H., Ausseur, J., Pinier, J., and Carlson, H., 2004 "Feedback Control of Separated Flows (Invited)". *AIAA Flow Control Conference*. Portland, OR.

[5] Pinier, J.T., Ausseur, J. M., Glauser, M. N. and Higuchi, H., 2007. "Proportional Closed-Loop Feedback Control of Flow Separation". *AIAA Journal*. Vol 45, No. 1, January.
[6] Camphouse, R.C., Myatt, J.H., Schmit, R.F., Glauser, M.N., Ausseur, J.M., Andino, M.Y., and Wallace, R.D., 2009 "A Snapshot Decomposition Method for Reduced Order Modeling and Boundary Feedback Control". *AIAA Flow Control Conference*. Seattle, WA.
[7] Wallace, R.D., Shea. P.R., Glauser, M.N., Vaithianathan, T., and Carlson, H.A., 2010 "Feedback Flow Control for a Pitching Turret (Part II)". *AIAA Paper 2010-361*. Orlando, FL.
[8] Fardad, M., 2009. On the Control of Flow Past a Disk. Sep.